

1 **O-GlcNAcylation of SAMHD1 Indicating a Link between Metabolic Reprogramming**
2 **and Anti-HBV Immunity**

3
4 **Running Title: O-GlcNAcylation of SAMHD1 inhibits HBV**
5

6 Jie Hu^{1, #}, Qingzhu Gao^{1, #}, Yang Yang^{1, #}, Jie Xia^{1, #}, Wanjun Zhang², Yao Chen¹, Zhi Zhou¹,
7 Lei Chang², Yuan Hu¹, Hui Zhou³, Li Liang¹, Xiaosong Li⁴, Quanxin Long¹, Kai Wang^{1, *},
8 Ailong Huang^{1, *}, Ni Tang^{1, *}

9 ¹Key Laboratory of Molecular Biology for Infectious Diseases (Ministry of Education),
10 Institute for Viral Hepatitis, Department of Infectious Diseases, The Second Affiliated
11 Hospital, Chongqing Medical University, Chongqing, China.

12 ²State Key Laboratory of Proteomics, Beijing Proteome Research Center, National Center
13 for Protein Sciences (Beijing), Beijing Institute of Lifeomics, Beijing, China.

14 ³School of Pharmaceutical Science, Chongqing Medical University, Chongqing, China.

15 ⁴The First Affiliated Hospital, Chongqing Medical University, Chongqing, China.

16

17 ***Correspondence**

18 Ni Tang, Ailong Huang, Kai Wang, Key Laboratory of Molecular Biology for Infectious
19 Diseases (Ministry of Education), Institute for Viral Hepatitis, Department of Infectious
20 Diseases, The Second Affiliated Hospital, Chongqing Medical University, Chongqing, China.

21 Phone: 86-23-68486780, Fax: 86-23-68486780,

22 E-mail: nitang@cqmu.edu.cn (N.T.), ahuang@cqmu.edu.cn (A.L.H.),
23 wangkai@cqmu.edu.cn (K.W.)

24 [#]These authors contributed equally to this work.

25 **Character count: 7465**

26 **Abstract**

27 Viruses hijack the host cell machinery to promote viral replication; however, the mechanism
28 by which metabolic reprogramming regulates innate antiviral immunity in the host remains
29 elusive. Herein, we found that Hepatitis B virus (HBV) infection upregulates glucose
30 transporter 1expression, promotes hexosamine biosynthesis pathway (HBP) activity, and
31 enhances O-linked β -N-acetylglucosamine (O-GlcNAc) modification of downstream proteins.
32 HBP-mediated O-GlcNAcylation positively regulates host antiviral response against HBV *in*
33 *vitro* and *in vivo*. Mechanistically, O-GlcNAc transferase (OGT)-mediated O-GlcNAcylation
34 of sterile alpha motif and histidine/aspartic acid domain-containing protein 1 (SAMHD1) on
35 Ser93 stabilizes SAMHD1 and enhances its antiviral activity. In addition, O-GlcNAcylation of
36 SAMHD1 promoted its antiviral activity against human immunodeficiency virus-1 *in vitro*. In
37 conclusion, the results of our study reveal a link between HBP, O-GlcNAc modification, and
38 innate antiviral immunity by targeting SAMHD1. Therefore, the results of this study
39 demonstrate a strategy for the potential treatment of HBV infection by modulating HBP
40 activity.

41

42 **Keywords:** Hepatitis B virus / O-linked β -N-acetylglucosamine modification / sterile alpha
43 motif and histidine/aspartic acid domain-containing protein 1 / antiviral immunity
44 /Hexosamine biosynthetic pathway

45 **Introduction**

46 Immunometabolism is an emerging field that highlights the importance of specific metabolic
47 pathways in immune regulation. Metabolic enzymes, such as glyceraldehyde 3-phosphate
48 dehydrogenase and pyruvate kinase isozyme M2 can directly modulate immune cell
49 activation (Chang *et al*, 2013; Palsson-McDermott *et al*, 2015). In addition to providing
50 energy and building blocks for biosynthesis, metabolites have been shown to participate in
51 epigenetic modification and signaling transduction. the glycolytic product lactate not only
52 regulates gene expression by histone acetylation (Zhang *et al*, 2019a), but also acts as a
53 suppressor of type I interferon signaling by interacting with the mitochondrial antiviral
54 signaling protein MAVS (Zhang *et al*, 2019b). Itaconate—another important metabolite for
55 immune function—downregulates type I interferon signaling during viral infection by
56 promoting alkylation of Kelch-like ECH-associated protein 1 and activation of
57 anti-inflammatory proteins, including nuclear factor erythroid 2-related factor 2 (Mills *et al*,
58 2018, 1; O'Neill & Artyomov, 2019).

59

60 Viruses are obligate parasites that rely on the biosynthetic machinery of the host to complete
61 their life cycle. They hijack the host cell machinery upon entry to fulfill their energetic and
62 biosynthetic demands for viral replication. Human cytomegalovirus (HCMV) and herpes
63 simplex virus-1 (HSV-1) remodel host cells to perform distinct, virus-specific metabolic
64 programs (Vastag *et al*, 2011). HCMV reprograms host metabolism by upregulating the
65 expression of carbohydrate-response element binding protein and glucose transporter 4
66 (GLUT4) to provide materials for viral replication(Yu *et al*, 2014).Glucose uptake, glycolysis,
67 and lipogenesis are enhanced in HCMV-infected cells to synthesize biomolecules. Moreover,
68 HSV-1 promotes central carbon metabolism to synthesize pyrimidine nucleotides.

69

70 On the other hand, hosts may recognize virus-induced signaling and reprogram metabolic
71 pathways to protect themselves from further damage. Increased glucose utilization,
72 increased aerobic glycolysis, and inhibition of oxidative metabolism have emerged as the
73 hallmarks of macrophage activation (Jung *et al*, 2019). Pattern recognition molecules as well
74 as several metabolic pathways and metabolites have been reported to play an important role
75 in regulating host innate immune response (Haskó & Cronstein, 2004; Skelly *et al*, 2019;
76 Tsalikis *et al*, 2013). Therefore, it is important to identify the key metabolites that regulate
77 innate immune response during viral infection. Understanding the relationship between cell
78 metabolism, innate immunity, and viral infection may provide insights to develop new
79 therapeutic targets to control viral infection.

80

81 Recent studies have emphasized the emerging role of the hexosamine biosynthesis
82 pathway (HBP)—a branch of glucose metabolism—in host innate immunity. HBP links
83 cellular glucose, glutamine, acetyl-CoA, and uridine triphosphate (UTP) concentrations with
84 signaling transduction(Hanover *et al*, 2012). Approximately 2–5% of the total glucose
85 entering a cell is converted to uridine diphosphate N-acetylglucosamine (UDP-GlcNAc)
86 (McClain & Crook, 1996)—the end-product of HBP—and serves as a donor for O-linked
87 β -N-acetylglucosamine (O-GlcNAc) modification (also known as O-GlcNAcylation) (Torres &
88 Hart, 1984). O-GlcNAc transferase (OGT) and O-GlcNAcase (OGA) are responsible for the
89 addition and removal of N-acetylglucosamine (GlcNAc) from Ser and Thr residues of target
90 proteins. Several key host proteins involved in immune modulation, including signal
91 transducer and activator of transcription-3 (STAT3), MAVS, and receptor-interacting
92 serine/threonine-protein kinase 3 (RIPK3), are targets for O-GlcNAcylation (Li *et al*, 2017,
93 2018, 2019a; Song *et al*, 2019). However, the mechanism by which HBP-mediated
94 O-GlcNAc modifications enhance antiviral innate immunity remains to be fully understood.

95

96 Hepatitis B virus (HBV) infection causes liver diseases, including acute and chronic hepatitis,
97 cirrhosis, and hepatocellular carcinoma, which is a major global public health concern (Tsai
98 *et al*, 2018). Current therapies improve both the quality of life and survival of patients with
99 hepatitis B. However, new therapeutic approaches are needed to achieve functional cure of
100 HBV infection (Fanning *et al*, 2019).

101

102 In this study, we investigated metabolic responses of host cells to HBV infection.
103 Our results show that HBP-mediated O-GlcNAcylation regulates the antiviral activity of
104 SAMHD1. Moreover, OGT promotes O-GlcNAcylation on Ser93 to enhance SAMHD1
105 stability and tetramerization, which is important for its antiviral activity. Our study established
106 a link between HBP, O-GlcNAc modification, and antiviral innate immunity by targeting
107 SAMHD1, thereby providing a potential drug target for treating HBV and human
108 immunodeficiency virus-1 (HIV-1) infection.

109

110 **Results**

111 **HBV infection upregulates GLUT1 expression and enhances HBP activity and protein**
112 **O-GlcNAcylation**

113 To explore metabolic changes in response to HBV infection, a metabolomics assay was
114 performed in AdHBV-1.3-infected HepG2 cells (HepG2-HBV1.3) and AdGFP-infected
115 HepG2 cells (HepG2-GFP). Principal component analysis showed that HBV infection
116 dramatically changes the intracellular metabolic profile of HepG2 cells (Fig. 1A). Several
117 metabolic pathways, including central carbon metabolism, amino sugar and nucleotide
118 sugar metabolism(Supplementary Fig.1A) were significantly affected. Recent studies have
119 shown that glucose metabolism plays a key role in host antiviral immunity (Li *et al*, 2018;
120 Song *et al*, 2019). Hence, we determined the effect of altering glucose metabolism in
121 HepG2-HBV1.3 cells. The expression level of several intermediate metabolites in glucose
122 metabolism, including 3-phospho-glycerate, GlcNAc, N-acetyl glucosamine 6- phosphate
123 (GlcNAc-6-P), and UDP-GlcNAc-the end-product of HBP-was increased upon HBV infection
124 (Fig. 1B-D). To confirm this result, we established a strain of HepG2 cells engineered to
125 express the human solute carrier family 10 member 1 (*SLC10A1*, also called NTCP) gene
126 (HepG2-NTCP cells), which allows them susceptible to HBV infection (Hu *et al*, 2019).
127 Targeted liquid chromatography-tandem mass spectrometry (LC-MS/MS) results showed a
128 significant increase in UDP-GlcNAc and glucose levels in HBV-infected HepG2-NTCP,
129 stable HBV-expressing HepAD38 (a tetracycline (Tet) inducible HBV expression cell line)
130 (Fig. 1E-F), and AdHBV-1.3-infected HepG2 (Supplementary Fig.1B-1C) cells. These results
131 were consistent with those observed in HepG2.2.15, an HBV-replicating cell line (Li *et al*,
132 2015). Because OGT-mediated protein O-GlcNAcylation is highly dependent on the
133 intracellular concentration of the donor substrate UDP-GlcNAc, we examined whether HBV
134 infection can affect O-GlcNAc modification in host cells. Total protein O-GlcNAcylation in

135 HBV-infected HepG2-NTCP cells significantly increased 6 to 9 days post HBV infection. A
136 similar result was observed in HepAD38 (Tet-off) cells (3 to 7 days after Tet removal from
137 the medium) (Fig. 1G). Further, GLUT1 expression was markedly enhanced in our HBV cell
138 models (Fig. 1H-I and Supplementary Fig.1D-E). Elevated glucose levels can increase HBP
139 flux and enhance UDP-GlcNAc synthesis (Housley *et al*, 2008). However, we did not
140 observe significant changes in the protein levels of OGT, OGA, and GFPT1—the key
141 enzymes that regulate HBP flux and protein O-GlcNAcylation (Supplementary
142 Fig.1F-G).These findings demonstrate that HBV infection upregulates GLUT1 expression,
143 promotes glucose uptake, and increases UDP-GlcNAc synthesis and protein
144 O-GlcNAcylation in host cells.

145

146 **Inhibition of protein O-GlcNAcylation promotes HBV replication in host cells**

147 Next, we evaluated the effects of protein O-GlcNAcylation on HBV replication. HBV-infected
148 HepG2-NTCP cells, HepAD38 (Tet-off) cells, and AdHBV-1.3-infected HepG2 cells were
149 treated with inhibitors of GLUT1, GFPT1, OGT, and OGA. Pharmacological inhibition of
150 GLUT1, GFPT1, and OGT reduced total protein O-GlcNAcylation levels (Fig. 2A-C,
151 Supplementary Fig. 2A-C and Supplementary Fig. 3A-C), and promoted HBV replication (Fig.
152 2D-I,Supplementary Fig. 2D-F and Supplementary Fig. 3D-F). Conversely, pharmacological
153 inhibition of OGA increased protein O-GlcNAcylation levels (Fig. 2J, Supplementary Fig. 2G
154 and Supplementary Fig. 3G) but suppressed HBV replication (Fig. 2K-L, Supplementary Fig.
155 2H and Supplementary Fig. 3H). These data suggest that HBP-mediated O-GlcNAcylation
156 positively regulates host antiviral immune response against HBV. The results of
157 pharmacological inhibitor studies were similar to those obtained from shRNA-mediated
158 knockdown of *GLUT1*, *GFPT*, *OGT*, or *OGA* in HepAD38 (Tet-off), HBV-infected
159 HepG2-NTCP, and AdHBV-1.3-infected HepG2 cells (Fig. 3 and Supplementary Fig. 4).

160 Taken together, these results indicate that inhibition of HBP or protein O-GlcNAcylation
161 promotes HBV replication, whereas increased O-GlcNAc modifications can enhance host
162 antiviral innate immune response against HBV.

163

164 **OGT mediates O-GlcNAcylation of SAMHD1 upon HBV infection**

165 To further investigate the mechanism by which OGT-mediated protein O-GlcNAcylation
166 promotes host antiviral innate immunity during HBV infection, we screened putative
167 O-GlcNAc-modified proteins in HepAD38 (Tet-off) cells using the immunoprecipitation assay
168 coupled with mass spectrometry (IP-MS). Cell lysates were immunoprecipitated with
169 O-GlcNAc antibodies and analyzed by LC-MS/MS. A total of 1,034 candidate
170 O-GlcNAc-modified proteins were identified (Supplementary Table 1). Gene ontology
171 analysis showed that several proteins were involved in innate immune and inflammatory
172 responses (Supplementary Fig. 5A). We next focused on SAMHD1, which plays an
173 important role in promoting host antiviral innate immunity (Ballana & Esté, 2015).
174 Interactions between OGT and SAMHD1 were demonstrated by co-immunoprecipitation
175 (co-IP) experiments in HepG2 cells (Fig. 4A-B). Confocal analysis indicated that OGT and
176 SAMHD1 are co-localized in the nucleus (Fig. 4C). We subsequently constructed three
177 SAMHD1 deletion mutants (Fig. 4D) and showed that the SAM domain of SAMHD1 is
178 required for its interaction with OGT (Fig. 4E). Immunoprecipitated Flag-tagged SAMHD1
179 exhibited a strong O-GlcNAc modification signal in HEK293 cells upon treatment with the
180 OGA inhibitor PUGNAc (Fig. 4F). Meanwhile, HBV replication enhanced SAMHD1
181 O-GlcNAcylation in HepAD38 (Tet-off) cells (Fig. 4G) and HBV-infected HepG2-NTCP cells
182 (Supplementary Fig. 5B). These results were further confirmed by affinity chromatography
183 using the succinylated wheat germ agglutinin (sWGA), a modified lectin that specifically

184 binds O-GlcNAc-containing proteins (Fig. 4H-I). Collectively, these data indicate that
185 SAMHD1 interacts with and can be O-GlcNAcylated by OGT upon HBV infection.

186

187 **OGT-mediated O-GlcNAcylation on Ser93 enhances SAMHD1 stability**

188 Next, we sought to map the O-GlcNAcylation site(s) on SAMHD1. Flag-tagged SAMHD1
189 was purified from HepG2-HBV1.3 cells and analyzed by MS. As shown in Fig. 4J, SAMHD1
190 was O-GlcNAcylated on Ser93 (S93). Interestingly, SAMHD1 S93 is well conserved among
191 mammalian species (Fig. 4K). We then generated site-specific point mutants of SAMHD1.
192 Mutation of S93 with Ala (S93A) largely reduced O-GlcNAc signal (Fig. 4L-M, and
193 Supplementary Fig. 5C). To further examine the effect of O-GlcNAcylation on SAMHD1
194 stability, Flag-tagged wild-type or S93A mutant SAMHD1 was overexpressed alone or with
195 shOGT in HepAD38 cells. The stability of exogenous SAMHD1 was decreased upon the
196 expression of shOGT or S93A mutant (Fig. 5A-D). Moreover, SAMHD1 stability and
197 ubiquitination was increased upon HBV infection (Fig. 5A-E). Furthermore, the
198 administration of PUGNAC dramatically suppressed total and K48-linked ubiquitination of
199 wild-type SAMHD1 (Fig. 5F); however, the effect on S93A ubiquitination was minimal (Fig.
200 5G). The S93A mutant was more ubiquitinated than wild-type SAMHD1 (Fig. 5G). These
201 data indicate that O-GlcNAcylation of SAMHD1 at Ser93 stabilizes SAMHD1 by preventing
202 its ubiquitination.

203

204 **O-GlcNAcylation of SAMHD1 on Ser93 enhances its antiviral activity**

205 It is known that the tetramer conformation of SAMHD1 is required for its dNTP
206 triphosphohydrolase (dNTPase) activity (Yan *et al*, 2013). Herein, we sought to determine
207 whether the S93A mutant affects SAMHD1 tetramerization and dNTPase activity.
208 Recombinant WT and S93A SAMHD1 were expressed and purified (Supplementary Fig.

209 6A-B). We found that S93A mutation destabilized SAMDH1 tetramers in HepAD38 cells (Fig.
210 6A) and reduced its dNTPase activity *in vitro* (Supplementary Fig. 6C-D). To test the effect of
211 S93 O-GlcNAcylation on SAMHD1 antiviral activity, we deleted endogenous SAMHD1 in our
212 HBV cell models and THP-1 cells using CRISPR-Cas9-mediated gene editing, and
213 transfected wild-type or SAMHD1 variants into SAMHD1-knockout HepAD38 (Tet-off) (Fig.
214 6B), AdHBV-1.3-infected HepG2 (Fig. 6C), and HepG2-NTCP cells. A phospho-mimetic
215 mutation (T592E) was used as a control that also decreased SAMHD1 dNTPase activity and
216 abrogated its antiviral activity (Sommer *et al*, 2016). Both southern blotting (Fig. 6B-C) and
217 qPCR (Fig. 6D-F) results indicated that S93A mutation impairs the ability of SAMHD1 to
218 inhibit HBV replication *in vitro*. A previous study showed that SAMHD1 dNTPase activity is
219 essential for HIV-1 restriction (Hansen *et al*, 2014). Therefore, we investigated the effect of
220 SAMHD1 O-GlcNAcylation on HIV-1 infection. THP-1 cells were infected with a vesicular
221 stomatitis virus G (VSV-G) protein pseudotyped HIV-1 molecular clone carrying the
222 luciferase gene reporter, and virus replication was assessed by quantifying luciferase activity.
223 Our results showed that protein O-GlcNAcylation was increased upon HIV-1 infection in
224 THP-1 cells (Fig. 6G). Subsequently, wild-type or SAMHD1 variants were transfected into
225 SAMHD1-KO THP-1 cells. S93A mutation also impaired the ability of SAMHD1 to restrict
226 HIV-1 replication in this single-round HIV-1 infection model (Fig. 6H). Treatment of cells with
227 the GFPT inhibitor 6-diazo-5-oxo-L-norleucine (DON) and the OGT inhibitor ST045849
228 significantly increased luciferase activity, whereas treatment with the OGA inhibitor PUGNAc
229 reduced luciferase activity (Fig. 6I). Taken together, these results indicate that
230 O-GlcNAcylation of SAMHD1 S93 promotes its antiviral activity *in vitro*.

231

232 **HBV infection promotes UDP-GlcNAc biosynthesis and O-GlcNAcylation *in vivo***

233 We used an HBV-transgenic (HBV-Tg) mouse model to verify our results *in vivo*
234 (Fig.7A).The level of O-GlcNAcylation was significantly higher in the liver tissues of HBV-Tg
235 mice than in those of normal C57BL/6 mice (Fig. 7B). Consistent with our *in vitro* data, the
236 administration of DON significantly reduced UDP-GlcNAc levels (Fig. 7C) and stimulated
237 HBV replication (Fig. 7D-F) in the mouse model of HBV infection, whereas the administration
238 of Thiamet G decreased serum HBV DNA (Fig. 7E), liver HBcAg (Fig. 7F) and HBV DNA
239 (Fig. 7G) levels in mice. Protein O-GlcNAcylation levels in the liver tissues of HBV-Tg mice
240 were increased upon Thiamet G administration, but decreased upon DON administration
241 (Fig. 7H). These results indicate that Thiamet G can promote host antiviral immunity by
242 increasing protein O-GlcNAcylation.Finally, we examined UDP-GlcNAc biosynthesis and
243 O-GlcNAcylation levels in patients with chronic hepatitis B (CHB). The levels of serum
244 UDP-GlcNAc (Fig. 7I), GLUT1 protein (Fig. 7J), and total O-GlcNAcylation (Fig. 7J and 7K)
245 were markedly higher in the liver tissues of patients with CHB than in those of normal
246 controls. In addition, SAMHD1 O-GlcNAcylation was significantly increased in the liver
247 tissues of the patients with CHB (Fig. 7K). Overall, our study suggests that HBV infection
248 upregulates GLUT1 expression and increases UDP-GlcNAc biosynthesis and
249 O-GlcNAcylation *in vivo*. As an essential O-GlcNAcylated protein, SAMHD1 can exert its
250 antiviral activity and elicit a robust host innate immune response against HBV infection.

251

252

253 **Discussion**

254 Although previous studies have demonstrated that HBV infection can alter glucose
255 metabolism in host cells, the role and underlying mechanisms of metabolic regulation of
256 antiviral immune responses remain elusive. In this study, we demonstrate that HBV
257 increases GLUT1 expression on hepatocyte surface, thereby facilitating glucose uptake.
258 This enhanced nutrient state consequently provides substrates to HBP to produce
259 UDP-GlcNAc, leading to an increase in protein O-GlcNAcylation. Importantly, we found that
260 pharmacological or transcriptional inhibition of HBP and O-GlcNAcylation can promote HBV
261 replication. Furthermore, we showed that OGT-mediated O-GlcNAcylation of SAMHD1 on
262 Ser93 is critical for its antiviral activity. Our results therefore indicate that O-GlcNAcylation
263 can positively regulate host antiviral immune response against HBV infection.

264

265 Similar to the metabolic reprogramming in proliferating cancer cells, virus reprogram host
266 cell metabolism. It has been reported that several viruses increase glucose consumption
267 and reprogram glucose metabolism in the host cell (Purdy & Luftig, 2019; Thaker *et al*, 2019).
268 GLUT1 expression was increased in host cells infected with HIV-1 (Loisel-Meyer *et al*, 2012;
269 Palmer *et al*, 2014), Kaposi's sarcoma-associated herpes virus (Gonnella *et al*, 2013),
270 dengue virus (Fontaine *et al*, 2015), and Epstein-Barr virus (Zhang *et al*, 2017). Our findings
271 are consistent with previous transcriptome-wide analyses, which have also shown
272 HBV-mediated upregulation of GLUT1 (Lamontagne *et al*, 2016). It has been suggested that
273 HBV pre-S2 mutant increases GLUT1 expression via mammalian target of rapamycin
274 signaling cascade, leading to enhanced glucose uptake (Teng *et al*, 2015, 2). However, the
275 precise molecular mechanism by which HBV upregulates GLUT1 remains poorly
276 understood.

277

278 The enhanced glucose uptake by glucose transporter not only accelerates glycolysis, but
279 may also increase flux into branch pathways, such as the pentose phosphate pathway and
280 HBP, which occur in cancer cells (Ma & Vosseller, 2014). Previous studies have reported
281 that HBP plays an important role in host innate immunity. Consistent with the results of a
282 previous study with HepG2.2.15 cells (Li *et al*, 2015), our results showed that HBV infection
283 can promote HBP activity and increase UDP-GlcNAc levels in different cell models. Li *et al*.
284 reported that enhanced HBP activity is essential for HBV replication because
285 pharmacological or transcription suppression of *GFPT1* inhibits HBV replication in
286 HepG2.2.15 cells. However, they did not use an *in vivo* HBV model to study the underlying
287 mechanism. In contrast, we showed that blockade of HBP promotes HBV replication,
288 whereas stimulation of HBP significantly suppresses HBV replication both *in vitro* and *in vivo*.
289 In addition, we observed similar results upon HIV-1 infection using a single-round infection
290 model. Although we could not exclude the possibility that differences between HBV cell
291 models cause this discrepancy, our results show that increased HBP flux and
292 hyper-O-GlcNAcylation can upregulate host antiviral innate response. Several other studies
293 have reported that HBP and/or protein O-GlcNAcylation promotes host antiviral immunity
294 against RNA viruses, including VSV (Li *et al*, 2018), influenza virus (Song *et al*, 2019), and
295 hepatitis C virus (Herzog *et al*, 2019). Thus, the present study confirms and expands our
296 current understanding of the antiviral activity of HBP and protein O-GlcNAcylation upon DNA
297 virus infection, which is similar to its antiviral activity upon infection by certain RNA viruses.
298
299 By characterizing the role of protein O-GlcNAcylation during HBV replication, we uncovered
300 SAMHD1 as an important target of OGT and established a link between O-GlcNAcylation
301 and antiviral immune response against HBV infection. SAMHD1, an effector of innate
302 immunity, can restrict most retroviruses (such as HIV-1) and several DNA viruses (including

303 HBV) by depleting the intracellular pool of dNTPs (Ballana & Esté, 2015). Several
304 post-translational modifications, including phosphorylation (White *et al*, 2013, 1) and
305 ubiquitination (Li *et al*, 2019b) have been reported to be critical for SAMHD1 function. Herein,
306 we identified Ser93 as a key O-GlcNAcylation site on SAMHD1 using LC-MS/MS.
307 Importantly, loss of O-GlcNAcylation by S93A mutation increased K48-linked ubiquitination,
308 thus decreased the stability and dNTPase activity of SAMHD1, suggesting that
309 O-GlcNAcylation promotes the antiviral activity of SAMHD1.

310

311 Because these results demonstrated the importance of protein O-GlcNAcylation in host
312 antiviral innate immunity against HBV, we proposed that an increase in SAMHD1
313 O-GlcNAcylation by inhibiting OGA activity could be used as a potential antiviral strategy.
314 This is in line with recent results indicating that increased MAVS O-GlcNAcylation is
315 essential to activate host innate immunity against RNA viruses (Li *et al*, 2018; Song *et al*,
316 2019). However, hyper-O-GlcNAcylation has been reported to stabilize several oncogenic
317 factors in several cancers associated with oncogenic virus infection (Makwana *et al*, 2019).
318 Human papillomavirus 16 E6 protein can upregulate OGT and stabilize c-MYC via
319 O-GlcNAcylation, thus promoting HPV-induced carcinogenesis (Zeng *et al*, 2016). Herzog *et*
320 *al.* demonstrated that protein O-GlcNAcylation is involved in HCV-induced disease
321 progression and carcinogenesis (Herzog *et al*, 2019). Thus, the role of protein
322 O-GlcNAcylation in HBV pathogenesis and the antiviral response through enhanced protein
323 O-GlcNAcylation remain to be further studied.

324

325 In conclusion, we uncovered a link between metabolic reprogramming and antiviral innate
326 immunity against HBV infection. We demonstrated that HBV infection upregulates GLUT1
327 expression and promotes HBP flux *in vitro* and *in vivo*. In addition, increased UDP-GlcNAc

328 biosynthesis and hyper-O-GlcNAcylation can enhance host antiviral innate response.

329 Mechanistically, OGT-mediated O-GlcNAcylation of SAMHD1 on Ser93 stabilizes SAMHD1

330 and enhances its antiviral activity (Fig. 7I). This study broadens our understanding of

331 SAMHD1 post-translational modification and provides new insights into the importance of

332 HBP and protein O-GlcNAcylation in antiviral innate immunity.

333

334 **Materials and Methods**

335 **Animal models**

336 HBV-transgenic (HBV-Tg) mice (n = 6 for each group) were kindly provided by Prof.
337 Ning-shao Xia, School of Public Health, Xiamen University(Huang *et al*, 2006). C57BL/6J
338 mice (6- to-8-week-old, six per group) were provided by the Laboratory Animal Center of
339 Chongqing Medical University (SCXK (YU) 2018-0003). Mice were intraperitoneally injected
340 with Don (1 mg/kg body weight), Thiamet G (20 mg/kg body weight), or PBS (control) every
341 other day for 10 times. On day 20 post-administration, mouse serum and liver tissue
342 specimens were collected for real-time PCR, southern blotting, and immunohistochemical
343 staining. Mice were treated in accordance with the guidelines established by the Institutional
344 Animal Care and Use Committee at the Laboratory Animal Center of Chongqing Medical
345 University. The animal care and use protocols adhered to the National Regulations for the
346 Administration of Laboratory Animals to ensure minimal suffering.

347

348 **Samples from patients with chronic hepatitis B virus infection**

349 The study protocol was approved by the Medical Ethics Committee of Chongqing Medical
350 University. Informed consent was obtained from patients who met the inclusion criteria for
351 chronic HBV infection.

352

353 **Metabolites analysis**

354 To extract metabolites from quenched serum/plasma samples or cell culture supernatants,
355 400 μ L chilled methanol: acetonitrile (2:2, v/v) was added to 100 μ L of each sample. The
356 mixture was vortexed three times for 1 min each with 5-min incubation at 4°C after each
357 vortexing step. After the final vortexing step of 30 s, the mixture was incubated on ice for 10
358 min. Thereafter, 100 μ L chilled HPLC-certified water was added to the samples, mixed for 1

359 min, and centrifuged at 13,000g for 10 min at 4°C. Finally, the liquid phase (supernatant) of
360 each sample was transferred into a new tube for UHPLC-QTOF-MS analysis in Shanghai
361 Applied Protein Technology Co., Ltd. UDP-GlcNAc and glucose were quantified using
362 targeted liquid chromatography-tandem mass spectrometry (LC-MS/MS). The data
363 acquisition, principal component analysis, heatmap and pathway impact analysis were
364 performed by Shanghai Applied Protein Technology Co., Ltd.

365

366 **Immunoprecipitation assay coupled with mass spectrometry (IP-MS)**

367 HepAD38 (Tet-off) cell lysates were incubated overnight with an anti-O-GlcNAc antibody at
368 4°C, followed by a 4-h incubation with protein A/G agarose beads. Immunoprecipitated
369 complexes were eluted and stained with Coomassie blue. Stained protein bands were sent
370 to Shanghai Applied Protein Technology Co., Ltd for identification of potential
371 O-GlcNAc-modified proteins. Protein bands were dissolved in 1 mL chilled methanol:
372 acetonitrile: H₂O (2:2:1, v/v/v) and sonicated at low temperature (30 min); this process was
373 repeated twice. The supernatant was dried in a vacuum centrifuge. For LC-MS analysis,
374 samples were re-dissolved in 100 µL acetonitrile: water (1:1, v/v). Sample analyses were
375 performed using a UHPLC system (1290 Infinity LC, Agilent Technologies) coupled to a
376 quadrupole time-of-flight analyzer (AB Sciex Triple TOF6600) at Shanghai Applied Protein
377 Technology Co., Ltd.

378

379 **SAMHD1 O-GlcNAcylation site mapping**

380 Mass spectrometry was performed to identify SAMHD1 O-GlcNAcylation sites, as described
381 previously (Peng *et al*, 2017). Briefly, immunoprecipitated SAMHD1 from HEK293T cells
382 was subjected to SDS-PAGE. The band corresponding to SAMHD1 was excised, digested
383 overnight with trypsin, and subjected to liquid chromatography-tandem mass spectrometry

384 (LC-MS/MS) analysis. An online LC-MS/MS setup consisting of an Easy-nLC system and an
385 Orbitrap Fusion Lumos Tribrid mass spectrometer (Thermo Scientific, Germany) equipped
386 with a nanoelectrospray ion source was used for all LC-MS/MS experiments. Raw MS files
387 were searched against the UniProt database using MaxQuant software (version 1.5.2.8).
388 The fixed modification was set to C (carbamidomethyl) and the variable modifications were
389 set to M (oxidation), protein N-term (acetyl), and S/T (O-GlcNAc). The peptide tolerance for
390 the first search was set at 20 ppm and that for the main search was set at 6 ppm. The
391 MS/MS tolerance was 0.02 Da. The false discovery level in PSM and protein was 1%. The
392 match between runs was used and the minimum score for modified peptides was set at 40.

393

394 **Statistical Analysis**

395 All data are expressed as the mean \pm standard deviation (SD). All statistical analyses were
396 performed using GraphPad Prism 5.0 software (GraphPad Software Inc.). Statistical
397 significance was determined using one-way ANOVA for multiple comparisons. Student's
398 *t*-test was used to compare two groups. $P < 0.05$ was considered statistically significant.

399

400 For detailed descriptions of other methods, please refer to **Supplementary Methods**.

401

402

403 **Acknowledgements**

404 We are grateful to Dr. T.-C He (University of Chicago, USA) for providing the pAdEasy
405 plasmid. We thank Prof. Bing Sun (Shanghai Institute of Biochemistry and Cell Biology,
406 China) for providing the pLL3.7 vector. We also thank Prof. Cheguo Cai (Wuhan University,
407 China) for providing the pNL4-3.Luc.R-E- plasmid. This work was supported by National
408 Natural Science Foundation of China (grant nos. 81872270, 81572683, 81661148057), the
409 Natural Science Foundation Project of Chongqing (cstc2018jcyjAX0254,
410 cstc2019jcyj-msxmX0587), the Major National S&T program (2017ZX10202203-004), the
411 National Key Research and Development Program of China (2018YFE0107500), the
412 Leading Talent Program of CQ CSTC (CSTCCXLJRC201719), and the Scientific Research
413 Innovation Project for Postgraduate in Chongqing (grant nosCYB19168, CYS19193)

414

415 **Authors Contributions**

416 NT, AH, and KW conceived the study and designed the experiments. JH, QG, YY and XJ
417 performed most experiments and analyzed the data. WZ and LC performed SAMHD1
418 O-GlcNAcylation site mapping. YC and ZZ collected clinical samples. LL generated
419 SAMHD1 mutants. QL assisted with HepG2-NTCP cell culture. YH, HZ and XL provided
420 guidance and advice. JH, QG, KW, and NT wrote the manuscript with all authors providing
421 feedback.

422

423 **Declaration of Interest**

424 The authors declare no competing interests.

425

426 **References**

- 427 Ballana E & Esté JA (2015) SAMHD1: At the Crossroads of Cell Proliferation, Immune
428 Responses, and Virus Restriction. *Trends Microbiol.* **23**: 680–692
- 429 Chang C-H, Curtis JD, Maggi LB, Faubert B, Villarino AV, O'Sullivan D, Huang SC-C,
430 van der Windt GJW, Blagih J, Qiu J, Weber JD, Pearce EJ, Jones RG & Pearce EL
431 (2013) Posttranscriptional Control of T Cell Effector Function by Aerobic Glycolysis.
432 *Cell* **153**: 1239–1251
- 433 Fanning GC, Zoulim F, Hou J & Bertoletti A (2019) Therapeutic strategies for hepatitis B
434 virus infection: towards a cure. *Nat. Rev. Drug Discov.* Available at:
435 <http://www.nature.com/articles/s41573-019-0037-0> [Accessed August 29, 2019]
- 436 Fontaine KA, Sanchez EL, Camarda R & Lagunoff M (2015) Dengue Virus Induces and
437 Requires Glycolysis for Optimal Replication. *J. Virol.* **89**: 2358–2366
- 438 Gonnella R, Santarelli R, Farina A, Granato M, D'Orazi G, Faggioni A & Cirone M (2013)
439 Kaposi sarcoma associated herpesvirus (KSHV) induces AKT hyperphosphorylation,
440 bortezomib-resistance and GLUT-1 plasma membrane exposure in THP-1 monocytic
441 cell line. *J. Exp. Clin. Cancer Res.* **32**: 79
- 442 Hanover JA, Krause MW & Love DC (2012) linking metabolism to epigenetics through
443 O-GlcNAcylation: Bittersweet memories. *Nat. Rev. Mol. Cell Biol.* **13**: 312–321
- 444 Hansen EC, Seamon KJ, Cravens SL & Stivers JT (2014) GTP activator and dNTP
445 substrates of HIV-1 restriction factor SAMHD1 generate a long-lived activated state.
446 *Proc. Natl. Acad. Sci.* **111**: E1843–E1851
- 447 Haskó G & Cronstein BN (2004) Adenosine: an endogenous regulator of innate immunity.
448 *Trends Immunol.* **25**: 33–39
- 449 Herzog K, Bandiera S, Pernot S, Fauville C, Jühling F, Weiss A, Bull A, Durand SC,
450 Chane-Woon-Ming B, Pfeffer S, Mercey M, Lerat H, Meunier J-C, Raffelsberger W,
451 Brino L, Baumert TF & Zeisel MB (2019) Functional microRNA screen uncovers
452 O-linked N-acetylglucosamine transferase as a host factor modulating hepatitis C
453 virus morphogenesis and infectivity. *Gut*: gutjnl-2018-317423
- 454 Housley MP, Rodgers JT, Udeshi ND, Kelly TJ, Shabanowitz J, Hunt DF, Puigserver P & Hart
455 GW (2008) O-GlcNAc Regulates FoxO Activation in Response to Glucose. *J. Biol.*
456 *Chem.* **283**: 16283–16292
- 457 Hu J, Lin Y-Y, Chen P-J, Watashi K & Wakita T (2019) Cell and Animal Models for Studying
458 Hepatitis B Virus Infection and Drug Development. *Gastroenterology* **156**: 338–354
- 459 Huang L-R, Wu H-L, Chen P-J & Chen D-S (2006) An immunocompetent mouse model for
460 the tolerance of human chronic hepatitis B virus infection. *Proc. Natl. Acad. Sci.* **103**:
461 17862–17867
- 462 Jung J, Zeng H & Horng T (2019) Metabolism as a guiding force for immunity. *Nat. Cell Biol.*
463 **21**: 85–93

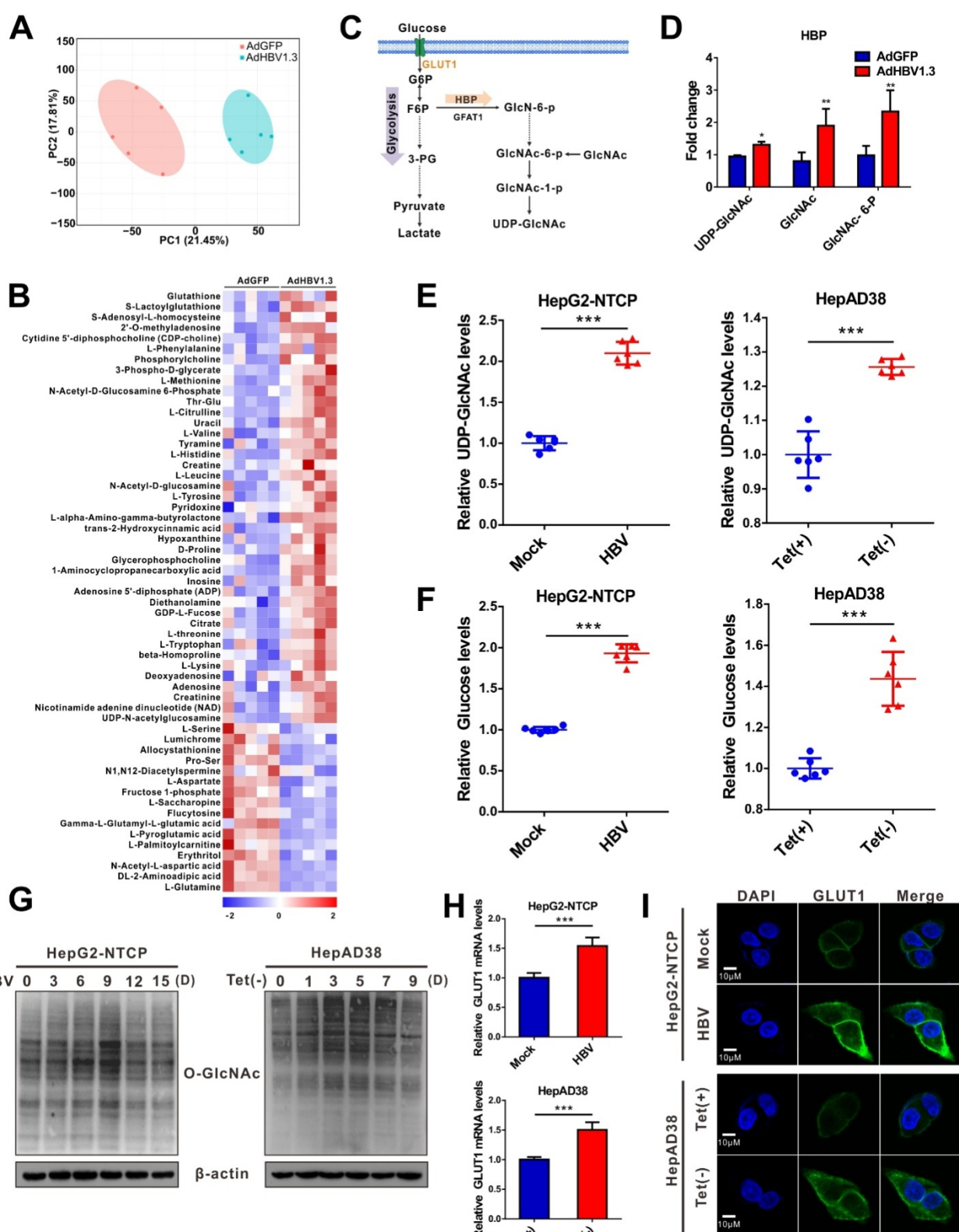
- 464 Lamontagne J, Mell JC & Bouchard MJ (2016) Transcriptome-Wide Analysis of Hepatitis B
465 Virus-Mediated Changes to Normal Hepatocyte Gene Expression. *PLOS Pathog.* **12**:
466 e1005438
- 467 Li H, Zhu W, Zhang L, Lei H, Wu X, Guo L, Chen X, Wang Y & Tang H (2015) The metabolic
468 responses to hepatitis B virus infection shed new light on pathogenesis and targets
469 for treatment. *Sci. Rep.* **5**
- 470 Li T, Li X, Attri KS, Liu C, Li L, Herring LE, Asara JM, Lei YL, Singh PK, Gao C & Wen H
471 (2018) O-GlcNAc Transferase Links Glucose Metabolism to MAVS-Mediated Antiviral
472 Innate Immunity. *Cell Host Microbe* **24**: 791-803.e6
- 473 Li X, Gong W, Wang H, Li T, Attri KS, Lewis RE, Kalil AC, Bhinderwala F, Powers R, Yin G,
474 Herring LE, Asara JM, Lei YL, Yang X, Rodriguez DA, Yang M, Green DR, Singh PK
475 & Wen H (2019a) O-GlcNAc Transferase Suppresses Inflammation and Necroptosis
476 by Targeting Receptor-Interacting Serine/Threonine-Protein Kinase 3. *Immunity* **50**:
477 576-590.e6
- 478 Li X, Zhang Z, Li L, Gong W, Lazenby AJ, Swanson BJ, Herring LE, Asara JM, Singer JD &
479 Wen H (2017) Myeloid-derived cullin 3 promotes STAT3 phosphorylation by inhibiting
480 OGT expression and protects against intestinal inflammation. *J. Exp. Med.* **214**:
481 1093–1109
- 482 Li Z, Huan C, Wang H, Liu Y, Liu X, Su X, Yu J, Zhao Z, Yu X-F, Zheng B & Zhang W (2019b)
483 TRIM21-mediated proteasomal degradation of SAMHD1 regulates its antiviral activity.
484 *EMBO Rep.* **n/a**: e47528
- 485 Loisel-Meyer S, Swainson L, Craveiro M, Oburoglu L, Mongellaz C, Costa C, Martinez M,
486 Cosset F-L, Battini J-L, Herzenberg LA, Herzenberg LA, Atkuri KR, Sitbon M, Kinet S,
487 Verhoeven E & Taylor N (2012) Glut1-mediated glucose transport regulates HIV
488 infection. *Proc. Natl. Acad. Sci.* **109**: 2549–2554
- 489 Ma Z & Vosseller K (2014) Cancer Metabolism and Elevated O-GlcNAc in Oncogenic
490 Signaling. *J. Biol. Chem.* **289**: 34457–34465
- 491 Makwana V, Ryan P, Patel B, Dukie S-A & Rudrawar S (2019) Essential role of
492 O-GlcNAcylation in stabilization of oncogenic factors. *Biochim. Biophys. Acta BBA -*
493 *Gen. Subj.* **1863**: 1302–1317
- 494 McClain DA & Crook ED (1996) Hexosamines and insulin resistance. *Diabetes* **45**:
495 1003–1009
- 496 Mills EL, Ryan DG, Prag HA, Dikovskaya D, Menon D, Zaslona Z, Jedrychowski MP, Costa
497 ASH, Higgins M, Hams E, Szpyt J, Runtsch MC, King MS, McGouran JF, Fischer R,
498 Kessler BM, McGettrick AF, Hughes MM, Carroll RG, Booty LM, et al (2018) Itaconate
499 is an anti-inflammatory metabolite that activates Nrf2 via alkylation of KEAP1. *Nature*
500 **556**: 113–117
- 501 O'Neill LAJ & Artyomov MN (2019) Itaconate: the poster child of metabolic reprogramming in
502 macrophage function. *Nat. Rev. Immunol.* **19**: 273–281
- 503 Palmer CS, Ostrowski M, Gouillou M, Tsai L, Yu D, Zhou J, Henstridge DC, Maisa A, Hearps

- 504 AC, Lewin SR, Landay A, Jaworowski A, McCune JM & Crowe SM (2014) Increased
505 glucose metabolic activity is associated with CD4+ T-cell activation and depletion
506 during chronic HIV infection. *AIDS Lond. Engl.* **28**: 297–309
- 507 Palsson-McDermott EM, Curtis AM, Goel G, Lauterbach MAR, Sheedy FJ, Gleeson LE,
508 van den Bosch MWM, Quinn SR, Domingo-Fernandez R, Johnston DGW, Jiang J,
509 Israelsen WJ, Keane J, Thomas C, Clish C, Vander Heiden M, Xavier RJ & O'Neill
510 LAJ (2015) Pyruvate Kinase M2 Regulates Hif-1 α Activity and IL-1 β Induction and Is
511 a Critical Determinant of the Warburg Effect in LPS-Activated Macrophages. *Cell
Metab.* **21**: 65–80
- 513 Peng C, Zhu Y, Zhang W, Liao Q, Chen Y, Zhao X, Guo Q, Shen P, Zhen B, Qian X, Yang D,
514 Zhang J-S, Xiao D, Qin W & Pei H (2017) Regulation of the Hippo-YAP Pathway by
515 Glucose Sensor O-GlcNAcylation. *Mol. Cell* **68**: 591-604.e5
- 516 Purdy JG & Luftig MA (2019) Reprogramming of cellular metabolic pathways by human
517 oncogenic viruses. *Curr. Opin. Virol.* **39**: 60–69
- 518 Skelly AN, Sato Y, Kearney S & Honda K (2019) Mining the microbiota for microbial and
519 metabolite-based immunotherapies. *Nat. Rev. Immunol.* **19**: 305–323
- 520 Sommer AFR, Rivière L, Qu B, Schott K, Riess M, Ni Y, Shepard C, Schnellbächer E,
521 Finkernagel M, Himmelsbach K, Welzel K, Kettern N, Donnerhak C, Münk C, Flory E,
522 Liese J, Kim B, Urban S & König R (2016) Restrictive influence of SAMHD1 on
523 Hepatitis B Virus life cycle. *Sci. Rep.* **6**: 26616
- 524 Song N, Qi Q, Cao R, Qin B, Wang B, Wang Y, Zhao L, Li W, Du X, Liu F, Yan Y, Yi W, Jiang
525 H, Li T, Zhou T, Li H, Xia Q, Zhang X, Zhong W, Li A, et al (2019) MAVS
526 O-GlcNAcylation Is Essential for Host Antiviral Immunity against Lethal RNA Viruses.
527 *Cell Rep.* **28**: 2386-2396.e5
- 528 Teng C-F, Hsieh W-C, Wu H-C, Lin Y-J, Tsai H-W, Huang W & Su I-J (2015) Hepatitis B Virus
529 Pre-S2 Mutant Induces Aerobic Glycolysis through Mammalian Target of Rapamycin
530 Signal Cascade. *PLoS ONE* **10**
- 531 Thaker SK, Ch'ng J & Christofk HR (2019) Viral hijacking of cellular metabolism. *BMC Biol.*
532 **17**: 59
- 533 Torres CR & Hart GW (1984) Topography and polypeptide distribution of terminal
534 N-acetylglucosamine residues on the surfaces of intact lymphocytes. Evidence for
535 O-linked GlcNAc. *J. Biol. Chem.* **259**: 3308–3317
- 536 Tsai K-N, Kuo C-F & Ou J-HJ (2018) Mechanisms of Hepatitis B Virus Persistence. *Trends
537 Microbiol.* **26**: 33–42
- 538 Tsalikis J, Croitoru DO, Philpott DJ & Girardin SE (2013) Nutrient sensing and metabolic
539 stress pathways in innate immunity. *Cell. Microbiol.* **15**: 1632–1641
- 540 Vastag L, Koyuncu E, Grady SL, Shenk TE & Rabinowitz JD (2011) Divergent Effects of
541 Human Cytomegalovirus and Herpes Simplex Virus-1 on Cellular Metabolism. *PLoS
542 Pathog.* **7**: e1002124

- 543 White TE, Brandariz-Nuñez A, Valle-Casuso JC, Amie S, Nguyen LA, Kim B, Tuzova M &
544 Diaz-Griffero F (2013) The Retroviral Restriction Ability of SAMHD1, but Not Its
545 Deoxynucleotide Triphosphohydrolase Activity, Is Regulated by Phosphorylation. *Cell*
546 *Host Microbe* **13**: 441–451
- 547 Yan J, Kaur S, DeLucia M, Hao C, Mehrens J, Wang C, Golczak M, Palczewski K,
548 Gronenborn AM, Ahn J & Skowronski J (2013) Tetramerization of SAMHD1 Is
549 Required for Biological Activity and Inhibition of HIV Infection. *J. Biol. Chem.* **288**:
550 10406–10417
- 551 Yu Y, Maguire TG & Alwine JC (2014) ChREBP, a glucose-responsive transcriptional factor,
552 enhances glucose metabolism to support biosynthesis in human
553 cytomegalovirus-infected cells. *Proc. Natl. Acad. Sci.* **111**: 1951–1956
- 554 Zeng Q, Zhao R-X, Chen J, Li Y, Li X-D, Liu X-L, Zhang W-M, Quan C-S, Wang Y-S, Zhai
555 Y-X, Wang J-W, Youssef M, Cui R, Liang J, Genovese N, Chow LT, Li Y-L & Xu Z-X
556 (2016) O-linked GlcNAcylation elevated by HPV E6 mediates viral oncogenesis. *Proc.*
557 *Natl. Acad. Sci.* **113**: 9333–9338
- 558 Zhang D, Tang Z, Huang H, Zhou G, Cui C, Weng Y, Liu W, Kim S, Lee S, Perez-Neut M,
559 Ding J, Czyz D, Hu R, Ye Z, He M, Zheng YG, Shuman HA, Dai L, Ren B, Roeder RG,
560 et al (2019a) Metabolic regulation of gene expression by histone lactylation. *Nature*
561 **574**: 575–580
- 562 Zhang J, Jia L, Lin W, Yip YL, Lo KW, Lau VMY, Zhu D, Tsang CM, Zhou Y, Deng W, Lung
563 HL, Lung ML, Cheung LM & Tsao SW (2017) Epstein-Barr Virus-Encoded Latent
564 Membrane Protein 1 Upregulates Glucose Transporter 1 Transcription via the
565 mTORC1/NF-κB Signaling Pathways. *J. Virol.* **91**: e02168-16
- 566 Zhang W, Wang G, Xu Z-G, Tu H, Hu F, Dai J, Chang Y, Chen Y, Lu Y, Zeng H, Cai Z, Han F,
567 Xu C, Jin G, Sun L, Pan B-S, Lai S-W, Hsu C-C, Xu J, Chen Z-Z, et al (2019b) Lactate
568 Is a Natural Suppressor of RLR Signaling by Targeting MAVS. *Cell* **178**: 176-189.e15
- 569

570 **Figures and Figure Legends**

Figure 1



571

572 **Fig. 1. HBV infection promotes HBP and increases protein O-GlcNAcylation**

573 (A) Principal component analysis of metabolite profiles obtained using a metabolomics

574 assay in HepG2 cells infected with AdHBV1.3 or AdGFP for 72 h.

575 (B) Heatmap of differentially expressed metabolites subjected to identical treatment

576 conditions as in (a). n = 5.

577 (C) An overview of the hexosamine biosynthesis pathway (HBP).

578 (D) Fold changes in the expression of differentially expressed intermediate metabolites of

579 HBP. n = 5.

580 (E-F) Fold change in the expression of UDP-GlcNAc (E) and glucose (F) in HBV-infected

581 HepG2-NTCP cells and HepAD38 cells with tetracycline inducible (Tet-off) HBV expression

582 was determined using the LC-MS/MS targeted metabolomics assay. n = 6.

583 (G) Immunoblot of total O-GlcNAc from HepG2-NTCP and HepAD38 cells treated for the

584 indicated periods.

585 (H-I) qPCR quantification (H) and immunofluorescence staining (I) of GLUT1 in

586 HepG2-NTCP and HepAD38 cells, DAPI (blue) was used to counterstain nuclei, n = 9. Scale

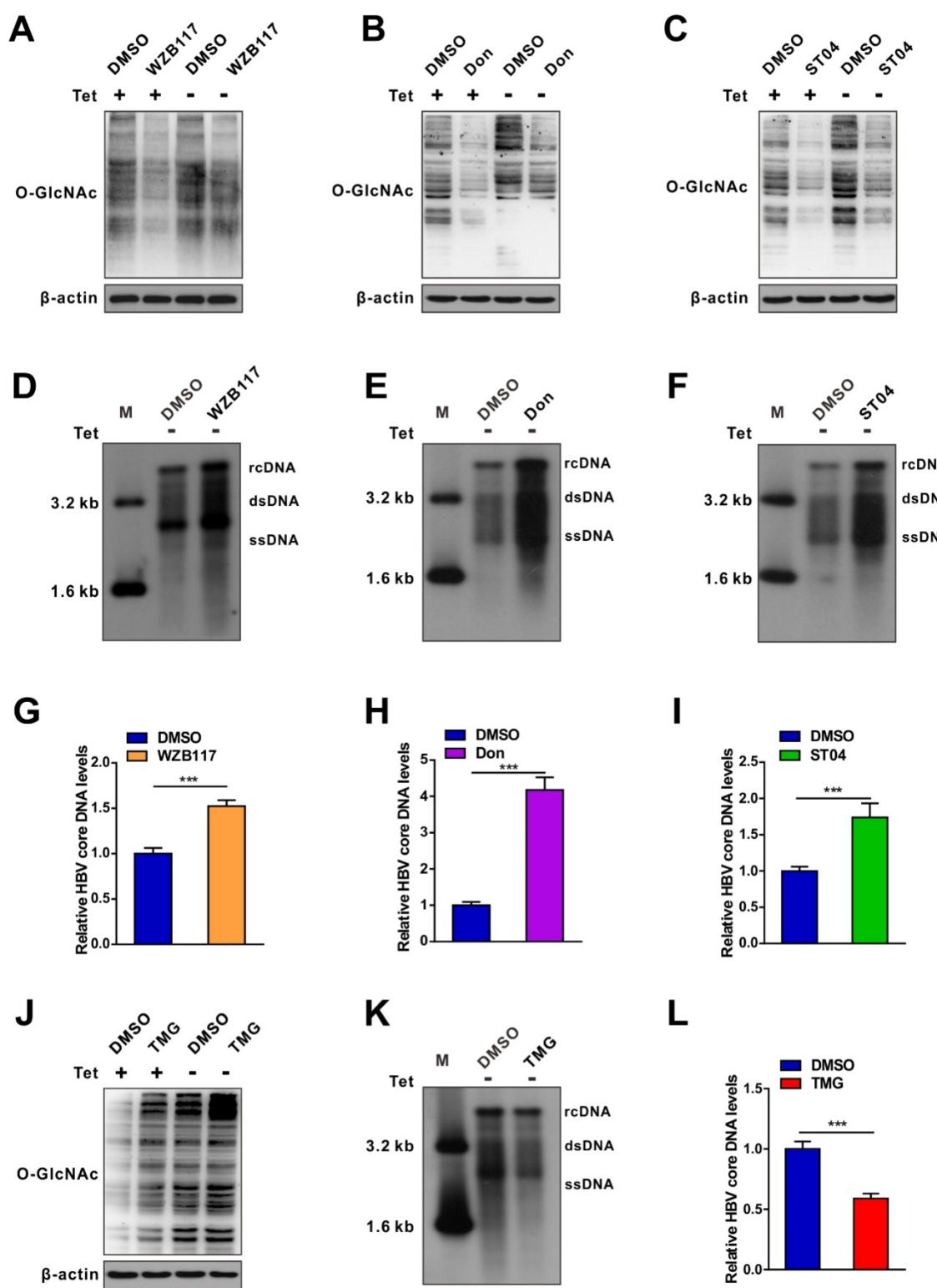
587 bar, 10 μ m.

588 Data are expressed as the mean \pm SD. P values were derived from unpaired, two-tailed

589 Student's *t*-test in E, F, and H; (** P < 0.001).

590

Figure 2



591
592 **Fig. 2. Pharmacological inhibition of protein O-GlcNAcylation promotes HBV
593 replication**

594 (A-C) Immunoblot of total O-GlcNAc from tetracycline-inducible HepAD38 cells treated with
595 or without GLUT1 inhibitor WZB117 (50 μ M) (A), GFPT1 inhibitor Don (30 μ M) (B), or OGT
596 inhibitor ST04 (100 μ M) (C) for 72 h. Don, 6-Diazo-5-oxo-L-norleucine; ST04, ST045849.
597 (D-F) HBV DNA were detected by Southern blot assay in stable HBV-expressing HepAD38
598 cells treated as above. rc DNA, relaxed circular DNA; ds DNA, double-stranded DNA; ss
599 DNA, single-stranded DNA.
600 (G-I) Quantification of HBV core DNA levels in stable HBV-expressing HepAD38 cells
601 treated as indicated using qPCR, n=9.
602 (J) Immunoblot of total O-GlcNAc from tetracycline-inducible HepAD38 cells treated with or
603 without OGA inhibitor TMG (100 μ M) for 72 h. TMG, Thiamet G.
604 (K-L) Southern blot analysis of HBV DNA and qPCR quantification of HBV core DNA levels
605 in stable HBV-expressing HepAD38 cells treated as in (J), n=9.
606 Data are expressed as the mean \pm SD. *P* values were derived from unpaired, two-tailed
607 Student's *t*-test in G-I and L; (***P*< 0.001).
608

Figure 3

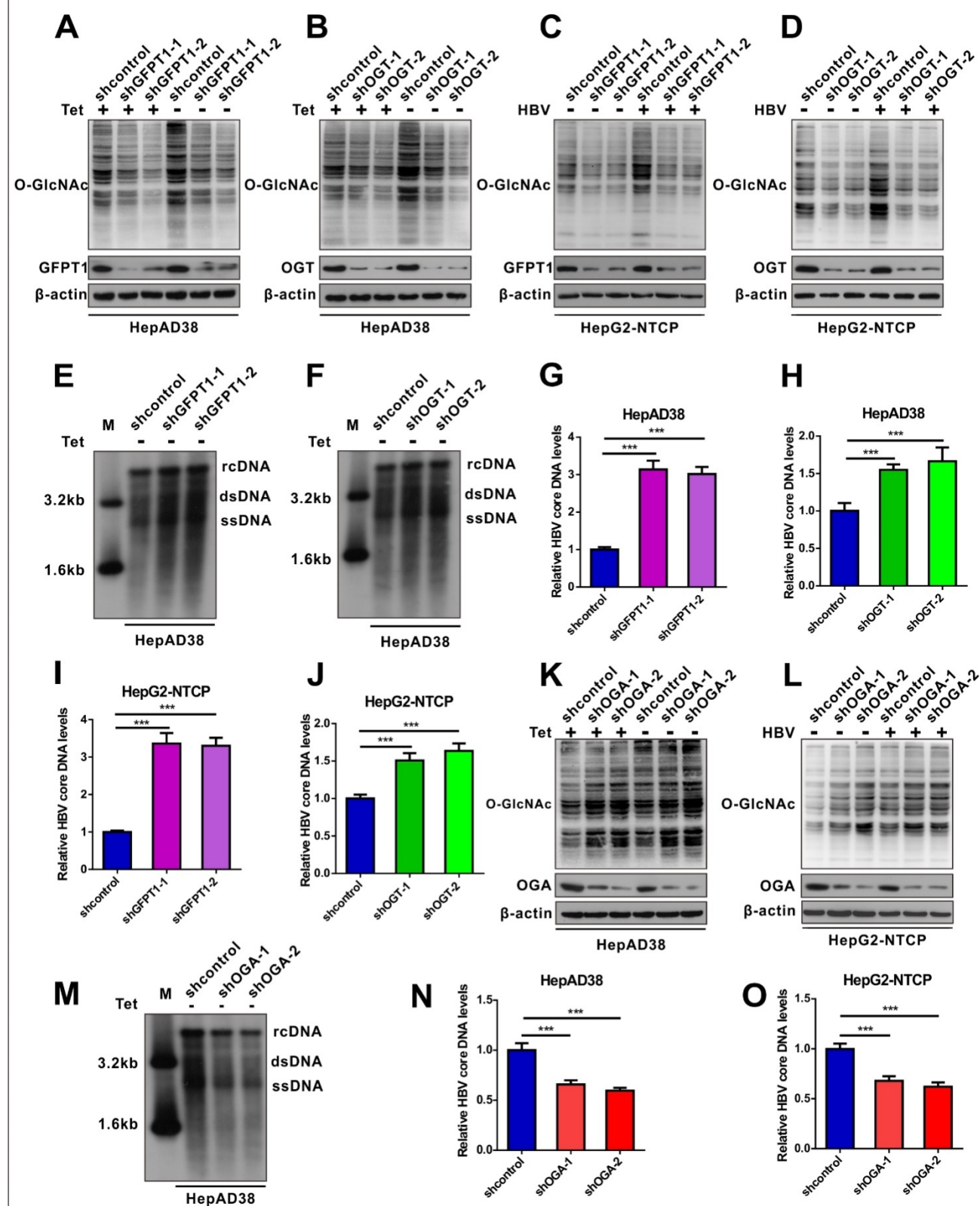


Fig. 3. shRNA-mediated inhibition of protein O-GlcNAcylation enhances HBV

609
610

611 replication

612 (A-D) Immunoblot of total O-GlcNAc from tetracycline-inducible HepAD38 cells (A-B) and
613 HBV-infected HepG2-NTCP cells (C-D) following shRNA-mediated knockdown of GFPT1
614 and OGT.
615 (E-H) Southern blot analysis of HBV DNA (E-F) and qPCR quantification of HBV core DNA
616 levels (G-H) in stable HBV-expressing HepAD38 cells treated as above, n=9.
617 (I-J) Quantification of HBV core DNA levels in HBV-infected HepG2-NTCP cells treated as
618 indicated using qPCR, n=9.
619 (K-L) Immunoblot of total O-GlcNAc from OGA-knockdown HepAD38 (Tet-off) cells (K) and
620 OGA-knockdown HBV-infected HepG2-NTCP cells (L).
621 (M) Southern blot analysis of HBV DNA in stable HBV-expressing HepAD38 cells treated as
622 in K.
623 (N-O) Quantification of HBV core DNA levels in stable HBV-expressing HepAD38 cells (N)
624 and HBV-infected HepG2-NTCP cells (O) treated as in (M) using qPCR, n=9.
625 Data are expressed as the mean \pm SD. *P* values were derived from one-way ANOVA in G-H,
626 I-J, and N-O; (***P*< 0.001).
627

Figure 4

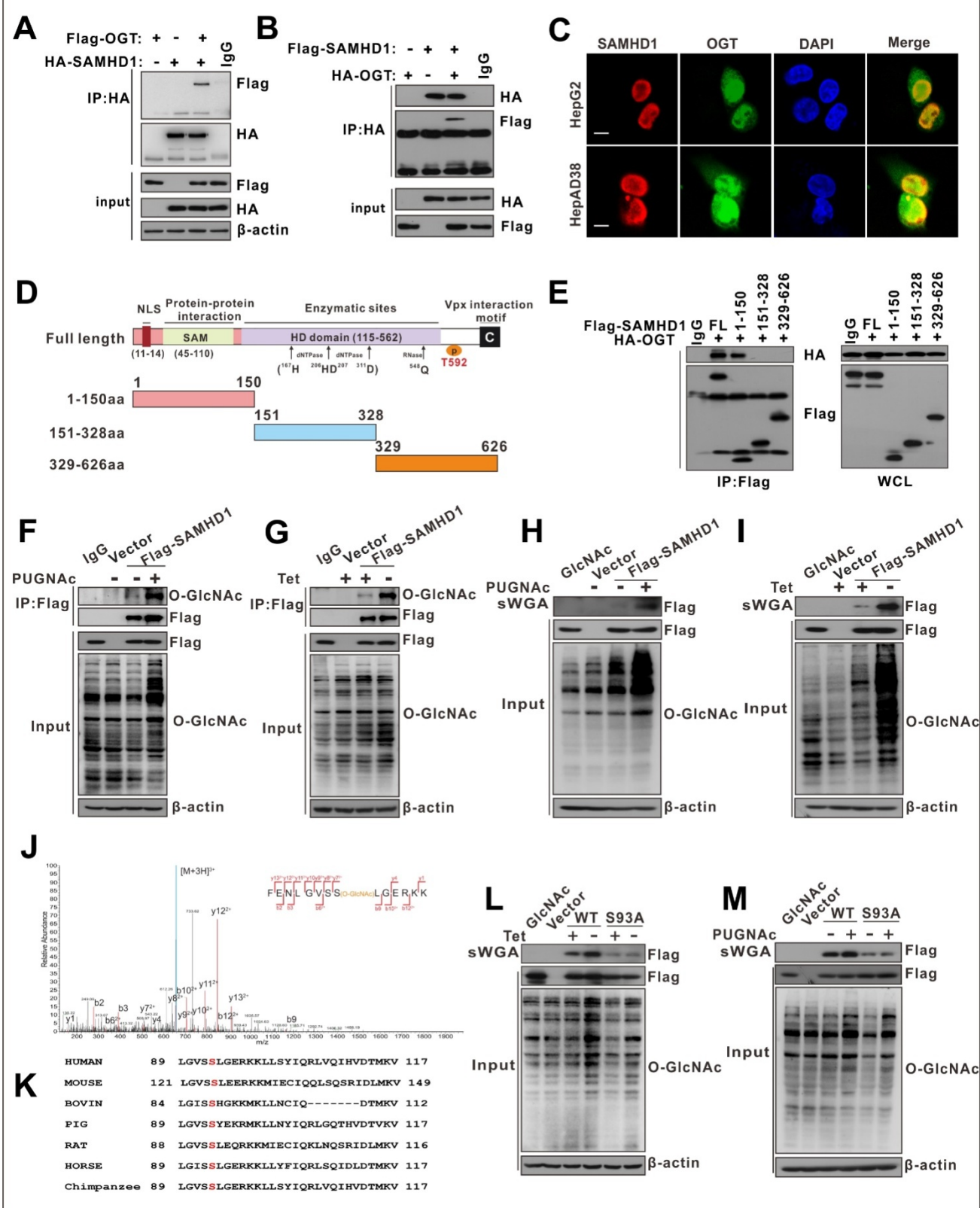


Fig. 4. OGT mediates O-GlcNAcylation of SAMHD1 on Ser93.

628

629

630 (A) Immunoprecipitation (IP) of SAMHD1 with anti-HA antibody in HEK293T cells

631 co-transfected with Flag-OGT and HA-SAMHD1 expression constructs. The
632 immunoprecipitated and input proteins were probed with the indicated antibodies.

633 (B) Immunoprecipitation of OGT with anti-HA antibody in HEK293T cells co-transfected with
634 HA-OGT and Flag-SAMHD1 expression constructs.

635 (C) Representative confocal images of HepG2 (top) and HepAD38 cells (bottom)
636 co-transfected with FLAG-SAMHD1 and HA-OGT. DAPI (blue) was used to counterstain
637 nuclei. Scale bar, 10 μ m.

638 (D-E) The interaction between OGT and the full-length or the truncated SAMHD1 (1-150aa,
639 151-328aa, 329-626aa), as indicated in the diagram (D), were determined by Co-IP in
640 HEK293T cells(E).

641 (F) HEK293T cells were transfected with the Flag-SAMHD1 construct and the control vector
642 for 48 h and treated with 100 μ M PUGNAc for 12 h. Following cell lysis, SAMHD1 was
643 immunoprecipitated using anti-FLAG M2 Agarose Beads. The immunoprecipitated and input
644 proteins were probed with an anti-O-GlcNAc or anti-Flag antibody.

645 (G) Immunoprecipitation of SAMHD1 with anti-Flag M2 agarose in tetracycline-inducible
646 HepAD38 cells transfected with Flag-SAMHD1 and the control vector.

647 (H-J) HEK293T cells (H) were treated as in (F) and tetracycline-inducible HepAD38 cells (I)
648 were treated as in (G). After cell lysis, O-GlcNAc-modified proteins were purified using
649 succinylated wheat germ agglutinin (sWGA)-conjugated agarose beads and probed with an
650 anti-Flag or anti-O-GlcNAc antibody. GlcNAc served as a negative control.

651 (J) LC-MS/MS analysis of FLAG-tagged SAMHD1 identified Ser93 as the SAMHD1
652 O-GlcNAcylation site. Tandem MS spectrum of the +2 ion at m/z 508.97 corresponding to
653 O-GlcNAcylated SAMHD1 peptide FENLGVSSLGERKK is shown.

654 (K) Multiple sequence alignment of SAMHD1 in different species.

655 (L-M) SAMHD1-KO HepAD38 cells were transfected with empty vector, Flag-tagged

656 SAMHD1 WT, or S93A mutant (l). HEK293T cells were transfected with the above plasmids
657 described in (L) and treated with 100 μ MPUGNAc for 12 h (M). Cell lysates were purified
658 using sWGA-conjugated agarose beads and probed with an anti-Flag or anti-O-GlcNAc
659 antibody.

660

Figure 5

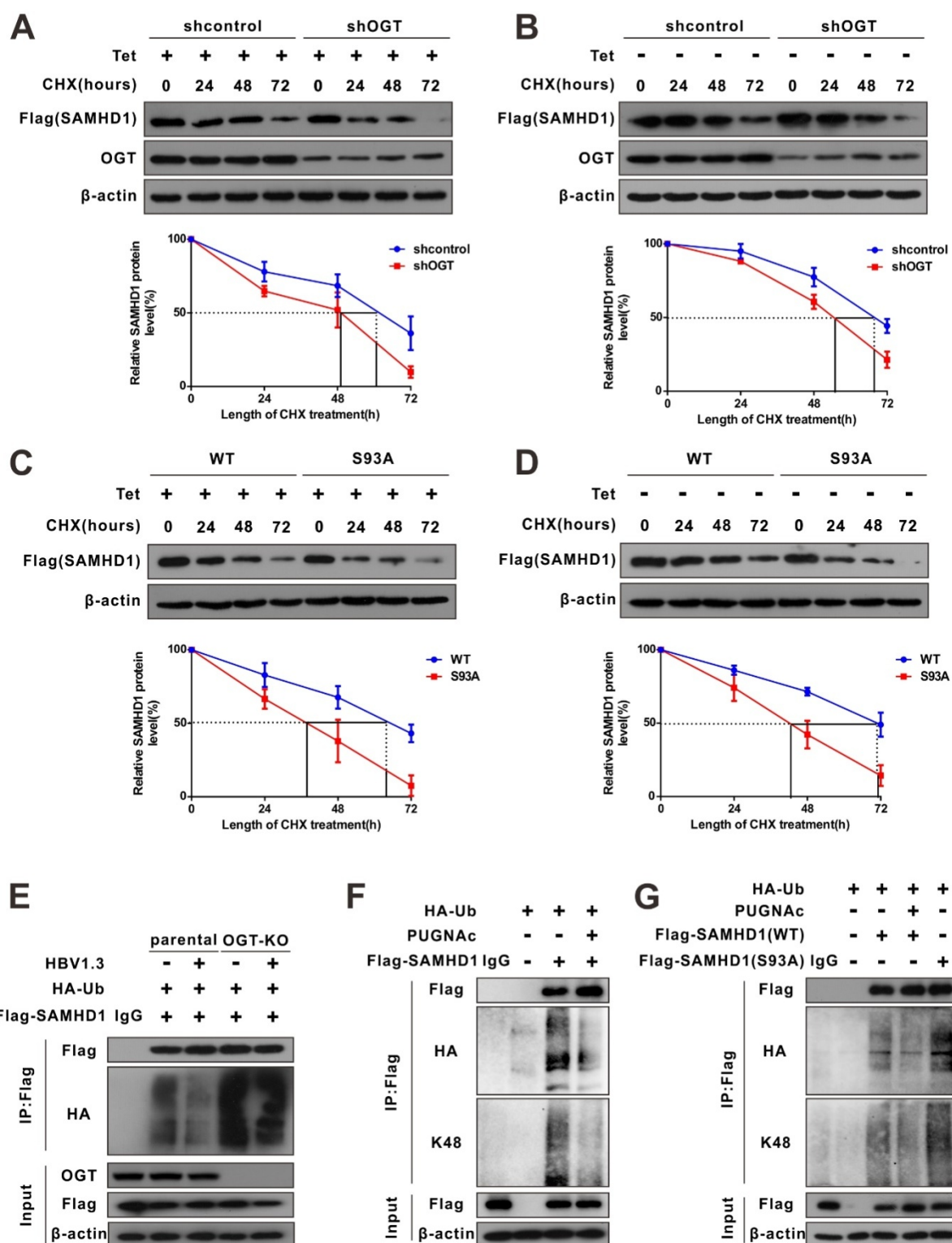


Fig. 5. OGT-mediated O-GlcNAcylation on Ser93 enhances SAMHD1 stability.

663 (A-B) Representative images of Flag-tagged SAMHD1 protein in non-infected or HBV

664 infected SAMHD1 KO HepAD38 cells. Cells were transfected with Flag-tagged SAMHD1
665 and treated with 100 μ M CHX for the indicated time. SAMHD1 band intensity was quantified
666 using ImageJ, n=3. CHX, Cycloheximide. KO, knockout.

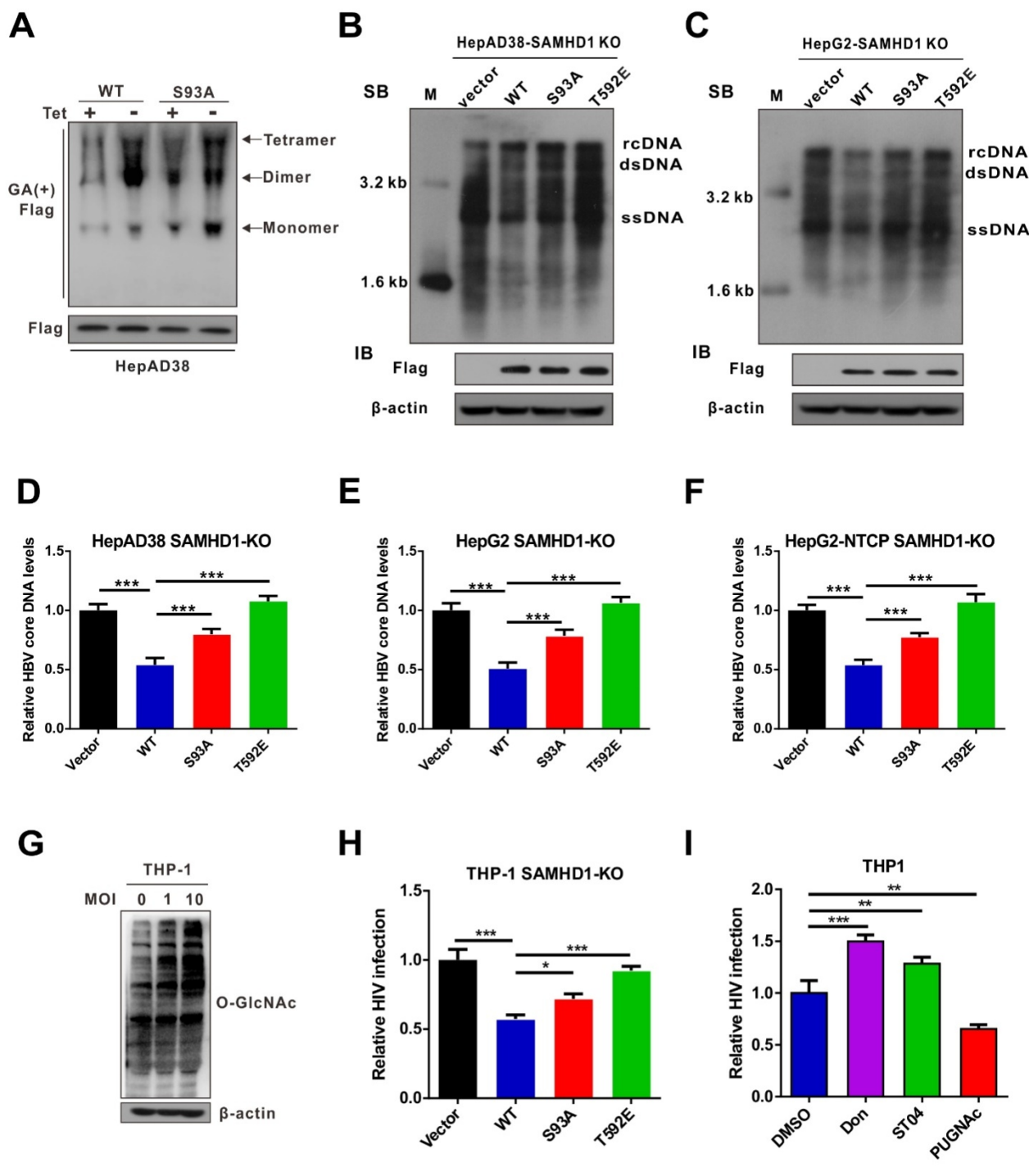
667 (C-D) Immunoblots of SAMHD1. SAMHD1-KO HepAD38 cells treated with (Off) or without
668 (On) tetracycline were transfected with Flag-tagged SAMHD1 WT or S93A mutant and
669 treated with 100 μ M CHX, n=3.

670 (E) SAMHD1 ubiquitination in OGT-knockout HBV-infected HepG2 cells in the presence of
671 HA-tagged ubiquitin. After cell lysis, SAMHD1 was immunoprecipitated using anti-FLAG M2
672 antibody. Immunoprecipitated and input proteins were probed with the indicated antibodies.

673 (F-G) HEK293T cells were co-transfected with HA-Ub and Flag-SAMHD1 (F), Flag-tagged
674 SAMHD1 WT or S93A mutant (G) and treated with 100 μ M PUGNAc for 12 h. After cell lysis,
675 SAMHD1 was immunoprecipitated using anti-FLAG M2 antibody. Immunoprecipitated and
676 input proteins were probed with the indicated antibodies.

677

Figure 6



678

679 **Fig. 6. O-GlcNAcylation of SAMHD1 on Ser93 is important for its antiviral activity**

680 **(A) Changes in the oligomeric state of SAMHD1 upon HBV infection. SAMHD1-KO**

681 HepAD38 cells with tetracycline inducible (Tet-off) HBV expression were transfected with the
682 Flag-tagged SAMHD1 WT or S93A mutant construct. Cells were treated with glutaraldehyde
683 (GA) and whole-cell lysates were probed with an anti-Flag antibody.

684 (B-C) HepAD38 cells with stable HBV-expressing (B) and HBV-infected SAMHD1-KO
685 HepG2 cells (C) were transfected with Flag-tagged SAMHD1 WT, S93A mutant, or T592E
686 mutant. HBV DNA levels were determined by southern blot analysis.

687 (D-F) SAMHD1-KO HepAD38 cells with stable HBV-expressing (D), HBV-infected
688 SAMHD1-KO HepG2 (E) and SAMHD1-KO HepG2-NTCP cells (F) were transfected with the
689 above plasmids described in (B). HBV core DNA levels were determined by qPCR. n=9.

690 (G) SAMHD1 KO-THP-1 cells were differentiated overnight with PMA (100 μ M) before
691 infecting with HIV-LUC-G (MOI=0, 1, or 10) for 48 h. Thereafter, the cells were lysed and
692 total O-GlcNAc levels were determined by western blotting. β -actin was used as a loading
693 control.

694 (H) SAMHD1 KO-THP-1 cells were differentiated overnight and infected with HIV-LUC-G
695 (MOI=1) for 24 h. Thereafter, they were transfected with Flag-tagged SAMHD1 WT, S93A
696 mutant, or T592E mutant for 48 h. Luciferase activity was measured and normalized for
697 protein concentration. n=3.

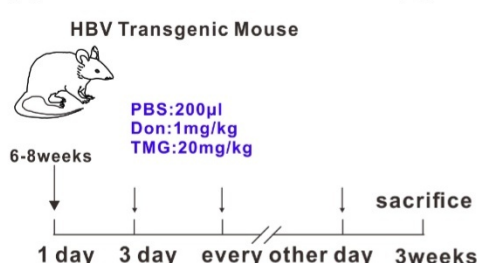
698 (I) SAMHD1 KO-THP-1 cells were differentiated overnight and infected with HIV-LUC-G
699 (MOI=1) for 24 h. Cells were then treated with Don (30 μ M, 24 h), ST04 (100 μ M, 24 h), or
700 PUGNAc (100 μ M, 48 h), and luciferase activity was measured. n=3.

701 Data are expressed as the mean \pm SD. *P* values were derived from one-way ANOVA in D-F,
702 H-I. (* *P*<0.05, ** *P*<0.01, ****P*<0.001).

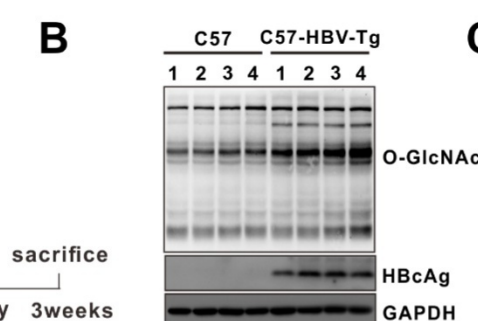
703
704

Figure 7

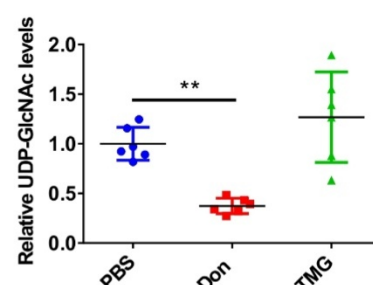
A



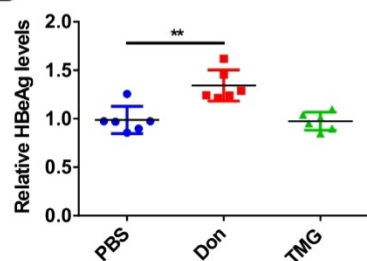
B



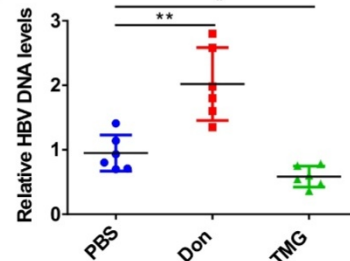
C



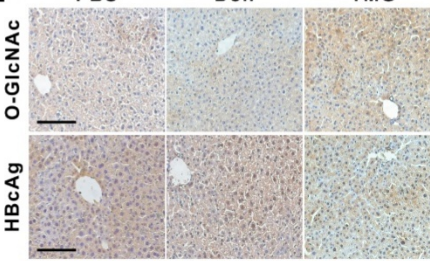
D



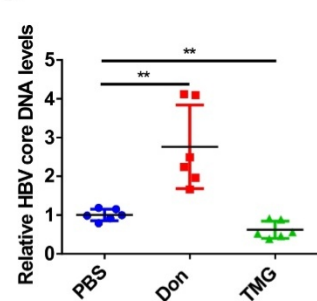
E



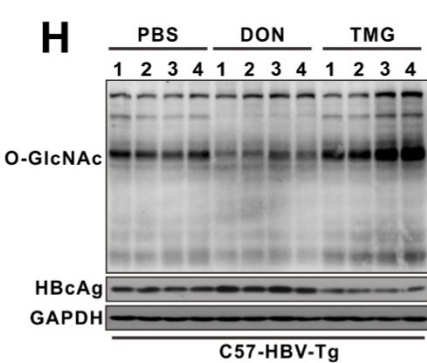
F



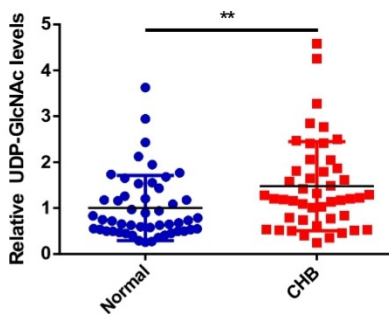
G



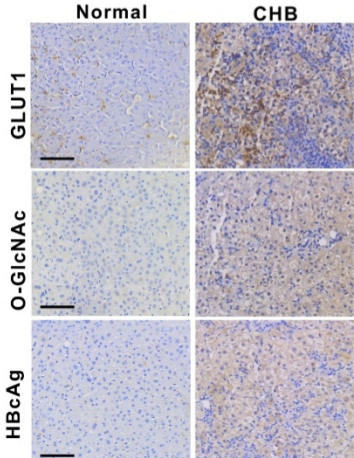
H



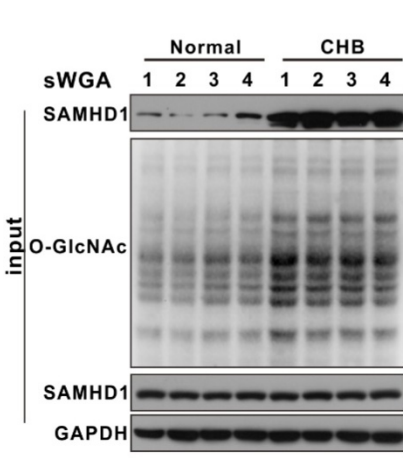
I



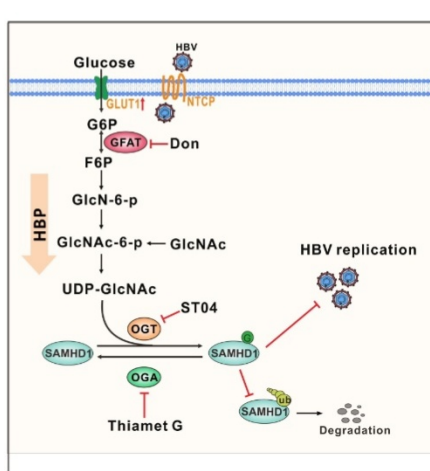
J



K



L



705
706

Fig. 7. HBV infection promotes UDP-GlcNAc biosynthesis and protein

707 **O-GlcNAcylation *in vivo***

708 (A) Six- to eight-week-old HBV transgenic mice were intraperitoneally injected with Don (1
709 mg/kg body weight) and TMG (20 mg/kg body weight) or PBS (control) every other day for
710 10 times. The mice were sacrificed on day 20 post-treatment.
711 (B) Immunoblotting of total O-GlcNAc in HBV transgenic mice.
712 (C) Fold change in the expression of UDP-GlcNAc in mouse liver tissues was determined by
713 UHPLC-QTOF-MS. n=6 per group.
714 (D-E) Serum HBeAg and HBV DNA levels in mice. n=6 per group.
715 (F) O-GlcNAc and HBcAg detection in mouse liver tissues, Scale bar, 50 μ m.
716 (G) Quantification of HBV core DNA levels in mouse liver tissues using qPCR. n=6.
717 (H) Immunoblot of total O-GlcNAc in HBV transgenic mice treated as in (A).
718 (I) Fold change in the expression of UDP-GlcNAc in the liver tissues of patients with CHB
719 was determined by UHPLC-QTOF-MS. (Normal=50, CHB=46).
720 (J) GLUT1, O-GlcNAc, and HBcAg detection in liver tissue specimens from patients with
721 CHB. Scale bar, 50 μ m.
722 (K) Liver tissue lysates from patients with CHB were purified using sWGA-conjugated
723 agarose beads and probed with an anti-SAMHD1 or anti-O-GlcNAc antibody.
724 (L) Proposed working model of this study.
725 Data are expressed as the mean \pm SD. *P* values were derived from one-way ANOVA in C-E,
726 G, and from unpaired, two-tailed Student's *t*-test in I. (* *P*<0.05, ** *P*< 0.01).
727
728